

# Realization of an atomically thin mirror using monolayer MoSe<sub>2</sub>

Patrick Back,<sup>1</sup> Aroosa Ijaz,<sup>1</sup> Sina Zeytinoglu,<sup>1</sup> Martin Kroner,<sup>1\*</sup> Atac Imamoglu<sup>1\*</sup>

<sup>1</sup>Institute for Quantum Electronics, ETH Zürich,  
CH-8093 Zurich, Switzerland

\*E-mail: mkroner@phys.ethz.ch or imamoglu@phys.ethz.ch

**Advent of new materials such as van der Waals heterostructures, propels new research directions in condensed matter physics and enables development of novel devices with unique functionalities. Here, we show experimentally that a monolayer of MoSe<sub>2</sub> embedded in a charge controlled heterostructure can be used to realize an electrically tunable atomically-thin mirror, that effects 90% extinction of an incident field that is resonant with its exciton transition. The corresponding maximum reflection coefficient of 45% is only limited by the ratio of the radiative decay rate to the linewidth of exciton transition and is independent of incident light intensity up to 400 Watts/cm<sup>2</sup>. We demonstrate that the reflectivity of the mirror can be drastically modified by applying a gate voltage that modifies the monolayer charge density. Our findings could find applications ranging from fast programmable spatial light modulators to suspended ultra-light mirrors for optomechanical devices.**

A plethora of ground-breaking experiments have established monolayers of transition metal dichalcogenides (TMD) such as MoSe<sub>2</sub> or WSe<sub>2</sub> as a new class of two dimensional (2D) direct

band-gap semiconductors [1, 2, 3, 4, 5]. In the absence of free carriers, the lowest energy elementary optical excitations in TMDs are excitons with an ultra-large binding energy of  $\sim 0.5$  eV [6]. While encapsulation of TMD monolayers with hexagonal boron nitride (hBN) leads to a reduction of the exciton binding energy [7, 8], it dramatically improves the optical quality, leading to an exciton line-broadening of  $\sim 2$  meV in photoluminescence (PL) or in absorption measurements [9, 10]. Remarkably, these narrow linewidths have a dominant contribution from radiative decay rate; the latter has been determined from exciton-polariton splitting in open cavity structures to be  $\sim 1.5$  meV for MoSe<sub>2</sub> [11, 12]. Motivated by these developments, we previously analyzed the optical response of a monolayer TMD theoretically and showed that it realizes an atomically-thin mirror [13].

Here, we present experiments demonstrating that an hBN encapsulated MoSe<sub>2</sub> monolayer has a reflection coefficient exceeding 40% and an extinction of resonant transmitted light of 90%. The combined reflection and transmission measurements allow us to conclude that the fraction of scattered light, stemming from inhomogeneous broadening of the exciton resonance, is less than 50%. Figure 1A shows a micrograph of the charge tunable heterostructure we have studied: a  $9\mu\text{m}$  by  $4\mu\text{m}$  MoSe<sub>2</sub> monolayer is sandwiched between two hBN layers. The heterostructure is placed on top of a transparent fused-silica substrate and capped with bilayer graphene. A gate voltage  $V_g$  applied between bilayer graphene and the MoSe<sub>2</sub> layer allows for tuning the electron density  $n_e$  [14, 15] and thereby modifying the resonance frequency as well as the nature of the elementary optical excitations [12].

Figure 1B depicts the outline of our experiments. We use near-resonant light to probe the excitonic excitations. To the extent that the MoSe<sub>2</sub> monolayer and its environment is homogeneous, in-plane momentum  $k$  is a good quantum number for both exciton and radiation field modes. In this limit, we use the input-output formalism of quantum optics to express the outgoing right-propagating electric field mode  $E_{\text{out}}^r(\omega)$  (Fig. 1B) in terms of the incident field modes

$E_{\text{in}}^{\text{r}}(\omega)$  and  $E_{\text{in}}^{\text{l}}(\omega)$  [13]

$$E_{\text{out}}^{\text{r}}(\omega) = \frac{\Gamma/2}{\Gamma/2 - i(\omega - \omega_{\text{exc}})} [(1 - \eta)E_{\text{in}}^{\text{r}}(\omega) - \eta E_{\text{in}}^{\text{l}}(\omega)], \quad (1)$$

where  $\omega_{\text{exc}}$  and  $\Gamma$  denote the transition frequency and the radiative decay rate of the excitons.  $\eta = \Gamma/\gamma_{\text{tot}}$  gives the ratio of radiative decay rate to the total (Lorentzian) exciton line broadening  $\gamma_{\text{tot}}$ . In our experiments  $E_{\text{in}}^{\text{r}}(\omega) = E_{\text{inc}} \neq 0$  whereas  $E_{\text{in}}^{\text{l}}(\omega) = 0$ ; in this limit the reflected and transmitted fields are given by  $E_{\text{refl}} = E_{\text{out}}^{\text{l}}(\omega)$  and  $E_{\text{trans}} = E_{\text{out}}^{\text{r}}(\omega)$ , respectively. The minimum and maximum (resonant) intensity transmission and reflection coefficients are given by  $T_{\text{min}} = (\gamma_{\text{tot}} - \Gamma)^2/\gamma_{\text{tot}}^2$  and  $R_{\text{max}} = \Gamma^2/\gamma_{\text{tot}}^2$ . Our formulation does not take into account small asymmetry in radiative decay rates into left and right propagating field modes stemming from the fused-silica substrate.

We measure the transmission and reflection spectrum of the heterostructure in a cryogenic transmission microscope with free space optical access as shown in Fig. 1C. The incident light is focussed to a diffraction limited spot with diameter  $\approx 700\text{nm}$ . For the excitation we use either a broad band light emitting diode (LED) centered at 780nm or a tunable single-mode Ti:S laser. Due to losses on the windows of the cryostat and the finite coupling/detection efficiency we can not directly measure the absolute reflected and transmitted power. Instead, we use a reference reflection and transmission spectrum of the incident light by moving our excitation spot off the MoSe<sub>2</sub> layer or off the heterostructure to the fused-silica layer.

Figure 2A shows the intensity reflection coefficient of light with a photon energy of 1.64 eV as we move the excitation/detection spot along the white line indicated in Fig. 1A. In the region around the blue spot, we measure the reflectivity of fused-silica layer; the extracted reflection coefficient of  $8 \pm 1\%$  (see Supplementary Materials) is in good agreement with 9.57% reflection we would expect from a thick fused-silica layer. Moving to the orange spot where we have the graphene/hBN heterostructure without the MoSe<sub>2</sub> monolayer, we observe a sizeable increase in

reflection coefficient to about  $28 \pm 5\%$ . Finally, reflection of the full heterostructure around the red spot exhibits very large variations in reflection coefficient ranging from 10% to more than 60%, demonstrating the ultra-strong optical response of monolayer MoSe<sub>2</sub>. Spatial variations in exciton resonance frequency, most likely stemming from inhomogeneous strain profile, result in the observed position dependent reflection coefficient of incident photons at a fixed frequency.

Figure 2B shows the normalized transmission spectrum obtained at the red spot, using a detection path numerical aperture (NA) of  $\sim 0.1$ . Even though the strong extinction of resonant light is evident, the dispersive nature of the transmission spectrum stemming from optical interference effects, does not allow us to read  $T_{\min}$  from the data directly. To extract the maximal extinction, we fit the data with a dispersive Lorentzian model (red curve). We find that a good fit is obtained for  $\gamma_{\text{tot}} = 3.6$  meV yielding an extinction coefficient of  $1 - T_{\min} = 0.76 \pm 0.15$ . We emphasize that extinction factors of this magnitude were previously only reported for transmon qubits coupled to superconducting microwave waveguides [16].

The reflection spectrum corresponding to the transmission data obtained at the red spot is depicted in Fig. 2C. The stronger asymmetry in reflection originates from an optical interference between two contributions with comparable magnitude – the excitonic emission and the incident light reflected from the heterostructure. The parameters used in the dispersive Lorentzian fit (red curve) to the reflection data using the same resonance energy and  $\gamma_{\text{tot}}$  as for the transmission spectrum, allows us to determine the maximal reflection coefficient of the MoSe<sub>2</sub> layer to be  $(46 \pm 9)\%$ . Remarkably, the sum of reflection and transmission, normalized to the corresponding value in the region around the orange spot, yields a symmetric but non-Lorentzian dip at the exciton resonance energy (Fig. 2C inset): the reduction of the total light intensity on resonance is a consequence of non-radiative line broadening and confirms that losses due to scattering into high  $k$  field modes or due to non-radiative recombination is less than 50%.

The aforementioned spatial inhomogeneity of the exciton resonance results in a variation

of not only the exciton resonance energy but also its linewidth across the sample. Figure 2D shows the dependence of the extracted resonant extinction coefficient on the linewidth of the exciton resonance, obtained by measuring transmission at different spots. We find that the broadened lineshapes are reasonably well fit by dispersive Lorentzians allowing us to compare the dependence of maximal extinction on total exciton linewidth ( $\gamma_{\text{tot}}$ ) to the theoretical value  $1 - (\gamma_{\text{tot}} - \Gamma)^2/\gamma_{\text{tot}}^2$ . This comparison in turn allows us to determine the radiative decay rate to be in the range  $1.4 \text{ meV} < \Gamma < 1.8 \text{ meV}$ , which is in good agreement with the values previously determined from normal-mode splitting of exciton-polaritons [11, 12]. We remark that at the locations yielding the highest observed extinction factor of  $\sim 0.9$ , we extract consistently higher values of  $\Gamma$ . However, at these points even the transmission spectrum exhibits strong asymmetry, rendering the extracted values less reliable.

Since the exciton-exciton interactions are proportional to the Bohr radius  $a_B$  [17], we would expect strongly bound TMD excitons with  $a_B \simeq 1 \text{ nm}$  to have a linear response to the incident field, provided that the induced exciton density  $n_{\text{exc}} \ll 1 \times 10^{12} \text{ cm}^{-2}$ . This argument in turn suggests that the response of this atomically-thin mirror should be independent of the incident light intensity  $I_L$  provided that  $I_L \ll 1 \times 10^5 \text{ Wcm}^{-2}$ . To verify this prediction, we used a single-mode Ti:S laser tuned into resonance with the  $\text{MoSe}_2$  exciton transition and monitored the dependence of extinction on the laser intensity. Figure 2E shows that the extinction indeed remains unchanged as we vary the incident intensity by 4 orders of magnitude from  $0.5 \text{ W/cm}^2$  to  $400 \text{ W/cm}^2$ . Verification of the theoretically predicted unusual saturation characteristics of TMD mirrors is likely to require pulsed laser excitation [13].

Due to strong exciton-electron interactions, the nature of elementary optical excitations can be drastically modified by applying  $V_g$  that modifies the free electron (or hole) density ( $n_e$ ) in the TMD monolayer [12]. A typical  $V_g$  dependent transmission spectrum is shown in Fig. S4 (Supplementary Materials): as  $n_e$  is increased a new attractive exciton-polaron resonance that is

red detuned by 25 meV with respect to the bare exciton transition emerges. The abrupt blue-shift and broadening of the exciton resonance for  $V_g > -2$  V on the other hand can be understood as the transition from a bare exciton into a repulsive-exciton-polaron resonance. In the context of our work, the  $V_g$  dependence of the optical response of the MoSe<sub>2</sub> monolayer indicates that the atomically-thin mirror can be electrically tuned.

Figure 3A shows the  $V_g$  dependence of maximal extinction coefficient obtained at exciton or repulsive-polaron resonance. The increase of minimum transmission from  $\sim 20\%$  down to  $90\%$  is due to a combination of electron-exciton interaction induced line broadening and oscillator strength transfer to attractive-polaron. If we instead focus on the response to incident photons at a specific energy, we find an even sharper drop in extinction from 0.6 down to 0.1 upon increasing  $V_g$  from  $-2$  V to  $0$  V, demonstrating electrical control of an atomically-thin mirror (Fig. 3A inset). With low resistance Ohmic contacts to the MoSe<sub>2</sub> monolayer, it should be possible to exploit the strong  $V_g$  dependence of excitonic response to realize fast switching of mirror transmission/reflection potentially on sub-ns timescales [18].

Due to the aforementioned oscillator strength transfer, maximal extinction at the attractive-polaron resonance first increases to about 0.2 before decreasing due to line broadening (Fig. 3B). Even though the optical response of the attractive polaron is relatively modest, its strong dependence on the valley polarization of electrons and its large g-factor exceeding 15 [19] render it an excellent candidate for realization of chiral optical devices.

The experiments shown in Fig. 2A-D as well as in Fig. 3A-B have been obtained by focusing the incident light onto a diffraction limited spot using a lens with  $NA = 0.68$  and then collecting the transmitted or reflected light with an  $NA \sim 0.1$ . This allowed us to monitor the optical response of excitons with  $k \sim 0$ . Figure 3C shows the dependence of maximal extinction for several values of the transmission path NA, close to the same spot we used to obtain the data depicted in Fig. 2B. We observe that as we increase transmission NA from 0.1 to 0.55, the

extinction drops from 0.9 down to 0.6 while the exciton linewidth increases from 2.5 meV to 3.5 meV. We attribute this strong NA dependence to electron-hole-exchange interaction induced modification of the exciton spectrum: it has been theoretically predicted that due to this interaction, the p-polarized excitons would have a Dirac-cone-like dispersion, leading to an energy splitting of s- and p-polarized excitons of order 3 meV for  $k \sim \omega_{\text{exc}}/c$  [20, 21]. To the best of our knowledge, the NA-dependent increase in linewidth that we report here provides the first direct evidence for this striking theoretical prediction.

The strong optical response of a TMD monolayer as demonstrated in our experiments opens up new avenues for photonics. On the one hand, the combination of ultra-light mass and high reflectivity suggests that these atomically-thin mirrors could revolutionize the performance of optomechanical mass and force sensors. On the other hand, the possibility to drastically modify reflection on ultra-short time scales on sub-wavelength length scales using applied electric fields could open up new perspectives for digital mirror devices or spatial light modulators. Last but not least, the valley degree of freedom of excitons and exciton-polarons can be used to realize chiral mirror devices by introducing a ferromagnetic monolayer next to the optically active TMD layer [22].

## References

- [1] B. Radisavljevic, A. Radenovic, J. Brivio, V. Giacometti, A. Kis, *Nat. Nanotechnol.* **6**, 147 (2011).
- [2] A. Splendiani, *et al.*, *Nano Lett.* **10**, 1271 (2010).
- [3] B. W. H. Baugher, H. O. H. Churchill, Y. Yang, P. Jarillo-Herrero, *Nat. Nanotechnol.* **9**, 262 (2014).
- [4] L. Britnell, *et al.*, *Science* **340**, 1311 (2013).

- [5] X. Xu, W. Yao, D. Xiao, T. F. Heinz, *Nature Physics* **10**, 343 (2014).
- [6] A. Chernikov, *et al.*, *Phys. Rev. Lett.* **113**, 076802 (2014).
- [7] S. Latini, T. Olsen, K. S. Thygesen, *Phys. Rev. B* **92**, 245123 (2015).
- [8] A. V. Stier, N. P. Wilson, G. Clark, X. Xu, S. A. Crooker, *Nano Lett.* **16**, 7054 (2016).
- [9] O. A. Ajayi, *et al.*, *arXiv* **1702.05857** (2017).
- [10] F. Cadiz, *et al.*, *arXiv* **1702.00323** (2017).
- [11] S. Dufferwiel, *et al.*, *Nat. Comm.* **6** (2015).
- [12] M. Sidler, *et al.*, *Nat. Phys.* **13**, 255 (2017).
- [13] S. Zeytinoglu, C. Roth, S. Huber, A. Imamoglu, *arXiv* **1701.08228** (2017).
- [14] J. S. Ross, *et al.*, *Nature Communication* **4**, 1474 (2013).
- [15] A. Chernikov, *et al.*, *Phys. Rev. Lett.* **115**, 126802 (2015).
- [16] A. F. van Loo, *et al.*, *Science* (2013).
- [17] C. Ciuti, V. Savona, C. Piermarocchi, A. Quattropani, P. Schwendimann, *Phys. Rev. B* **58**, 7926 (1998).
- [18] D. Krasnozhan, D. Lembke, C. Nyffeler, Y. Leblebici, A. Kis, *Nano Letters* **14**, 5905 (2014).
- [19] P. Back, *et al.*, *arXiv* **1701.01964** (2017).
- [20] H. Y. anf Gui-Bin Liu, P. Gong, X. Xu, W. Yao, *Nat. Comm.* **5** (2014).
- [21] D. Y. Qiu, T. Cao, S. G. Louie, *Phys. Rev. Lett.* **115**, 176801 (2015).



[22] B. Huang, *et al.*, *arXiv* **1703.05892v2** (2017).

## **Acknowledgments**

This work is supported by an ERC Advanced investigator grant (POLTDES), Spin-NANO Marie Skłodowska-Curie Grant Agreement No. 676108 and NCCR QSIT.

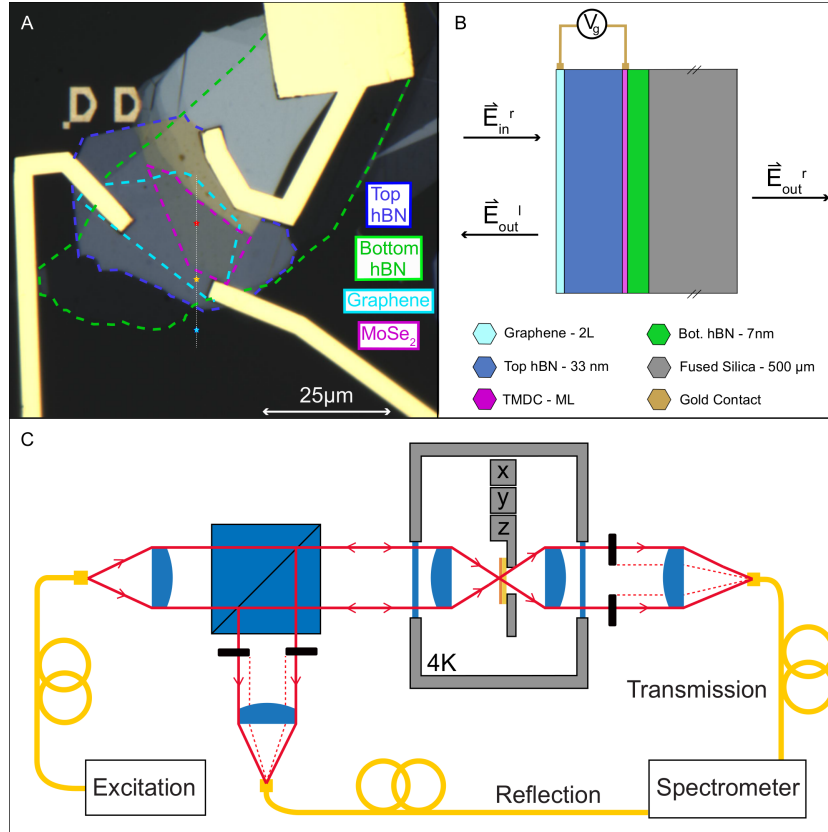


**Figure 1: A gate controlled van der Waals heterostructure in a confocal setup.** (A) Micrograph of the measured heterostructure: the MoSe<sub>2</sub> monolayer is encapsulated in between 33 nm (top) and 7 nm (bottom) thick hBN layers, which are indicated by blue and green dashed lines. To allow for optical transmission measurements the heterostructure is transferred on to a transparent 500µm thick fused-silica substrate. To achieve charge control of the MoSe<sub>2</sub>, the heterostructure is capped by a graphene bilayer. The graphene and the MoSe<sub>2</sub> are electrically contacted by titanium/gold electrodes. The white line and colored stars indicate the position of optical measurements on and off the MoSe<sub>2</sub> and the hBN layers. (B) Illustration of the interaction of an incident field with a MoSe<sub>2</sub> monolayer. Optical fields can be characterized as consisting of right propagating input  $E_r^{in}$  and right and left propagating output modes  $E_r^{out}$ ,  $E_l^{out}$  respectively. (C) The schematic of the experimental setup. The sample is mounted in a Helium flow cryostat in between two aspheric lenses in confocal configuration. The sample can be moved in situ by piezo stepper motors. A collimated excitation beam is focussed onto the sample by the first lens. The reflected light is collimated again by the same lens (NA= 0.68). The transmitted light is collimated by the second lens (NA=0.55). By reducing the diameter of the collection beam we can reduce the effective NA of the detection optics, thereby reducing the spread in the in-plane momentum  $k$  of the detected photons. Since the excitation paths remain unchanged, we only excite a small area of the sample which guarantees little excess inhomogeneous broadening due to disorder of the flake even for a small detection NA.

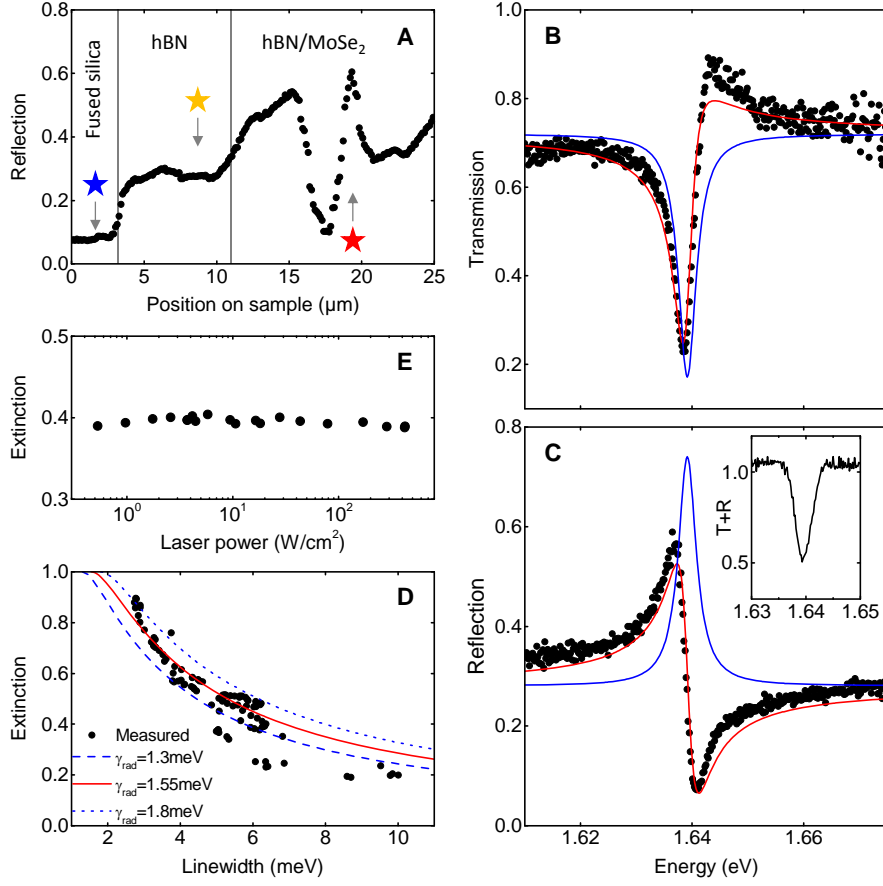


**Figure 2: Resonant optical response of a MoSe<sub>2</sub> monolayer.** (A) The measured reflection coefficient at a photon energy of 1.64eV across the white line indicated in Fig.1A. The reflection increases from 8% in the fused-silica region (blue star) to about 28% in the region having both top and bottom hBN layers as well as bilayer graphene (yellow star). The strong variations in reflection between 12 $\mu$ m and 25 $\mu$ m stems from the position dependence of the exciton resonance of the MoSe<sub>2</sub>. The incident photons are resonant with the exciton transition at the position indicated by the red star. (B) Transmission as function of photon energy of the MoSe<sub>2</sub>/hBN heterostructure measured at the position indicated by the red star with a detection arm numerical aperture of 0.1. The black dots represent the normalized data (see Supplementary Materials). The red line is a fit to the data using a dispersive Lorentzian model yielding  $\gamma_{\text{tot}} = 3.6$ meV. The blue line shows the corresponding Lorentzian, indicating an extinction coefficient of 0.76. (C) Reflection as function of photon energy measured under identical conditions as in (B). The fit allows us to extract resonant reflection enhancement by a factor of 1.67, indicating that the maximum reflectivity of the MoSe<sub>2</sub> monolayer is 46%. The inset shows the sum of the transmission and reflection spectra. (D) Demonstration of linewidth dependence of maximal extinction. The black dots show the extracted extinction on resonance ( $1 - T_{\text{min}}$ ) as function of the measured linewidth  $\gamma_{\text{tot}}$ . The lines indicate the dependence of the extinction as function of  $\gamma_{\text{tot}}$  for different radiative decay rates  $\Gamma$ . (E) Extinction of a single-mode laser resonant with the exciton transition as function of its intensity. 11

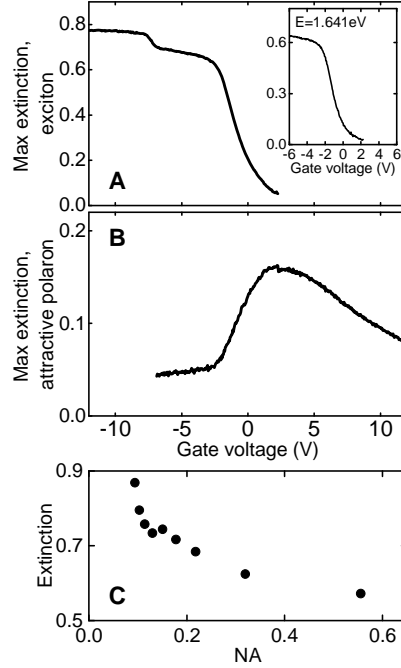


Figure 3: **Electrical control of an atomically-thin mirror.** (A) Gate voltage ( $V_g$ ) dependence of the maximal extinction of transmitted light using the exciton resonance. Injection of free carriers reduces the exciton oscillator strength and increases linewidth, leading to a sharp  $V_g$  dependent drop in transmission. The inset shows the extinction of incident photons with a fixed energy of 1.641eV as function of  $V_g$  demonstrating that transmission can be changed from 10% to 60% by changing  $V_g$  by  $\sim 2$  V. (B)  $V_g$  dependence of maximal extinction at the attractive exciton-polaron resonance: the extinction increases with increasing electron density until  $V_g \sim 2$  V due to oscillator strength transfer from the exciton resonance. For  $V_g > 2$  V, excess line broadening suppresses the resonant enhancement of optical response. (C) Measured maximal extinction as function of the NA of the detection optics. Increasing NA leads to an increase of the linewidth and a corresponding reduction of extinction. The observations are consistent with electron-hole exchange interaction induced splitting of s- and p-polarized excitonic resonances which, in the absence of polarization selection, leads to line broadening.

**Supplementary Materials for**  
**Realization of an atomically thin mirror using monolayer MoSe<sub>2</sub>**

Patrick Back,<sup>1</sup> Aroosa Ijaz,<sup>1</sup> Sina Zeytinoglu,<sup>1</sup> Martin Kroner,<sup>1\*</sup> Atac Imamoglu<sup>1\*</sup>

<sup>1</sup>Institute for Quantum Electronics, ETH Zürich,  
CH-8093 Zurich, Switzerland

\*To whom correspondence should be addressed;

E-mail: mkroner@phys.ethz.ch or imamoglu@phys.ethz.ch

**I. MEASUREMENT SETUP**

The sample investigated in the main text is a monolayer MoSe<sub>2</sub> flake, encapsulated in between two hBN layers. The monolayer is gate tunable thanks to bilayer graphene placed on the top hBN. The sample was transferred onto a 0.5 mm thick transparent fused-silica substrate using a dry transfer method [1]. Using atomic force microscope (AFM) measurements we estimate the surface roughness of the substrate to be about  $\Delta t = 10$  nm. The hBN layer between the MoSe<sub>2</sub> flake and the bilayer graphene has a thickness of  $t_1 \simeq 33$  nm and the hBN between the MoSe<sub>2</sub> and the fused-silica has a thickness of  $t_2 \simeq 7$  nm. An AFM image of the main text sample and the corresponding line-cut used to determine the thicknesses is shown in Fig. S1. The sample is contacted using titanium/gold and can be doped by applying a voltage between the bilayer graphene and the MoSe<sub>2</sub> monolayer. For the measurements, the device was mounted in a flow cryostat with free space optical front and back access.

**II. CAPACITIVE MODEL FOR THE FERMI ENERGY**

The electron density  $n_e$  of the gated monolayer MoSe<sub>2</sub> sample can be tuned by applying a gate voltage  $V_g$  between the bilayer graphene and the MoSe<sub>2</sub> monolayer. From Fig. S2, we estimate the gate voltage for which we start populating the lowest energy conduction band to be  $V_g = -8$  V. For the gate dependent extinction measurements shown in Fig. S4, the injected  $n_e$  appears to remain constant at a value  $\ll 1 \times 10^{12}$  cm<sup>-2</sup> in the gate voltage range  $-8$  V  $< V_g < -2$  V: the characteristic sharp blue-shift of the exciton resonance, along with the substantial oscillator strength transfer to the attractive polaron resonance is observed in the range  $V_g > -2$  V in Fig. S4.

The capacitance per unit area  $C/A$  between bottom gate and sample is given by:

$$\frac{C}{A} = \left( \frac{t_{\text{hBN}}}{\epsilon_{\text{hBN}}\epsilon_0} + \frac{1}{e^2 D(E)} \right)^{-1}, \quad (1)$$

with  $D(E)$  denoting the density of states of the monolayer. The structure used for the experiments shown in the main text has an hBN layer with thickness  $t_{\text{hBN}} \simeq 33$  nm and static (perpendicular) dielectric constant  $\epsilon_{\text{hBN}} \approx 3$ . Therefore, for this structure  $L/\epsilon = t_{\text{hBN}}/\epsilon_{\text{hBN}} = 11$  nm. The second term in the expression, the quantum capacitance, can be neglected as long as the Fermi energy lies within the conduction or valence band.

### III. PHOTOLUMINESCENCE AND TRANSMISSION MEASUREMENTS

We took gate dependent photoluminescence (PL) measurements from the sample depicted in the main text. A typical gate dependent PL measurement is shown in Fig. S2. The excitation laser wavelength was 714 nm. We note that the resonance energy/wavelength varies across the sample. This can be verified by comparing the resonance wavelengths of Fig. S2 and S3 that were obtained on two different spots on the same sample.

Figure S4 shows a color coded plot of back gate (BG) voltage dependent transmission spectrum. For low BG voltages when the sample has low electron densities, there is high extinction at the exciton resonance frequency. By increasing the BG voltage,  $n_e$  is increased and we reach a regime where we get sizeable extinction at the attractive exciton-polaron resonance.

### IV. NORMALIZATION OF REFLECTION AND TRANSMISSION SPECTRA

In order to obtain the reflection and transmission coefficients of the sample we measure both integrated transmitted  $I_t$  and reflected  $I_r$  power across the sample (along the white line shown in Fig. 1A of the main text). From these measurements we extract values for the transmitted (reflected) power on the the fused-silica  $I_{t,\text{fs}}$  ( $I_{r,\text{fs}}$ ) and the hBN  $I_{t,\text{hBN}}$  ( $I_{r,\text{hBN}}$ ) but off the MoSe<sub>2</sub> flake. We assume that

$$1 = R_{\text{fs}} + T_{\text{fs}} = \alpha_r I_{r,\text{fs}} + \alpha_t I_{t,\text{fs}}, \quad (2)$$

$$1 = R_{\text{hBN}} + T_{\text{hBN}} = \alpha_r I_{r,\text{hBN}} + \alpha_t I_{t,\text{hBN}}. \quad (3)$$

Here,  $\alpha_r$  and  $\alpha_t$  account for the losses of the detection system in the reflection and transmission arm, respectively. Our experimental accuracy is insufficient to measure directly the influence of the bilayer graphene on the transmitted or reflected power on the hBN.

We find  $R_{\text{fs}} = 0.076 \pm 0.015$  and  $R_{\text{hBN}} = 0.28 \pm 0.06$  and the corresponding values for the transmission coefficients.  $R_{\text{fs}}$  corresponds well with the expected reflection coefficient of the fused-silica substrate (0.096). A matrix transfer calculation of reflection coefficient of the hBN/fused-silica layer structure using the layer thicknesses obtained by AFM however requires a refractive index of  $n \sim 2.5$  for the hBN to yield the experimentally observed value. The measured reflection coefficient for an excitation energy of 1.6391eV is plotted in Fig. 2A of the main text.

In order to obtain the spectrum of the reflection and transmission coefficients of the MoSe<sub>2</sub>/hBN/fused-silica heterostructure we record a transmission  $T_{\text{on}}$  and reflection  $R_{\text{on}}$  spectrum, for a given electron density or detection NA on the MoSe<sub>2</sub>/hBN/fused-silica heterostructure (position indicated by the red dot in Fig. 1A of the main text). Typical spectra obtained this way are plotted using black dots in Fig. S5A for transmission and Fig. S5B for reflection, measured at  $V_g = 10V$  and  $NA = 0.1$ . For normalization we take a reference spectrum off the MoSe<sub>2</sub> monolayer but still on the bilayer graphene, the top hBN and the bottom hBN layer (orange star in Fig. 1A of the main text) in transmission  $T_{\text{off}}$  and reflection  $R_{\text{off}}$  (red dots in Fig. S5 A and B). We calculate the TMD monolayer transmission and reflection coefficient at each photon energy as

$$T = \frac{T_{\text{on}}/T_{\text{off}}}{T_{\text{hBN}}}, \quad (4)$$

$$R = \frac{R_{\text{on}}/R_{\text{off}}}{R_{\text{hBN}}}. \quad (5)$$

## V. RESULTS FROM OTHER SAMPLES

We carried out transmission measurements on 4 different samples. The results across all samples differed only in magnitude depending on exciton linewidth. Fig. S6 shows the 68% extinction seen in one of the samples without charge control. Although the line widths observed in this sample were broader than the main sample, the general relation between the amount of extinction and resonance linewidth (see inset of Fig. S6 ) is similar to that shown in Fig. 2D of the main text.

- 
- [1] P. J. Zomer, M. H. D. Guimares, J. C. Brant, N. Tombros, and B. J. van Wees, Applied Physics Letters **105**, 013101 (2014).

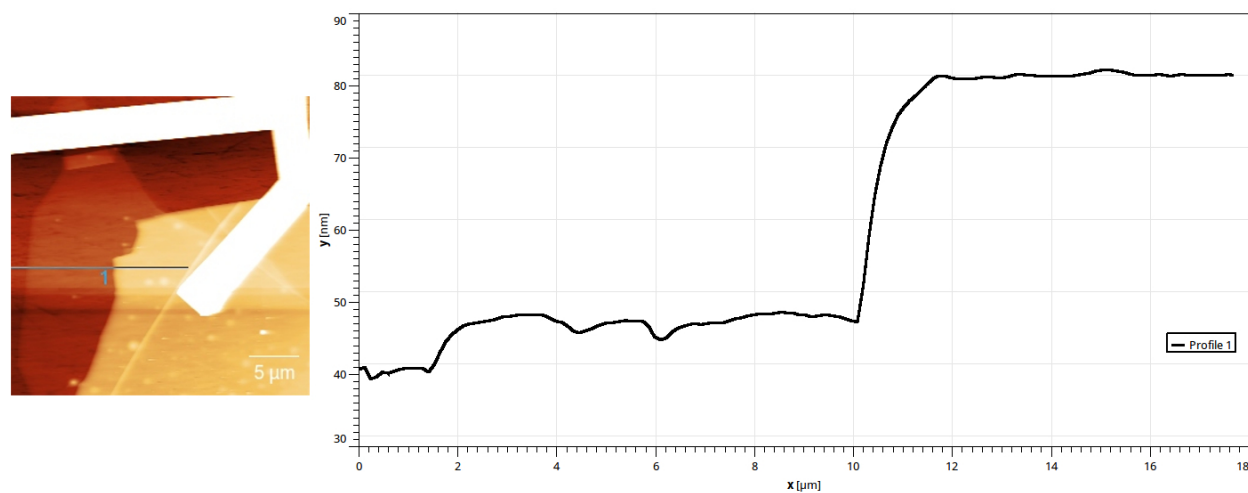


FIG. S1: AFM image taken on the sample of the main text. From the line profile, we estimate the bottom and top hBN layers to have a thickness of  $\simeq 7$  nm and  $\simeq 33$  nm, respectively.



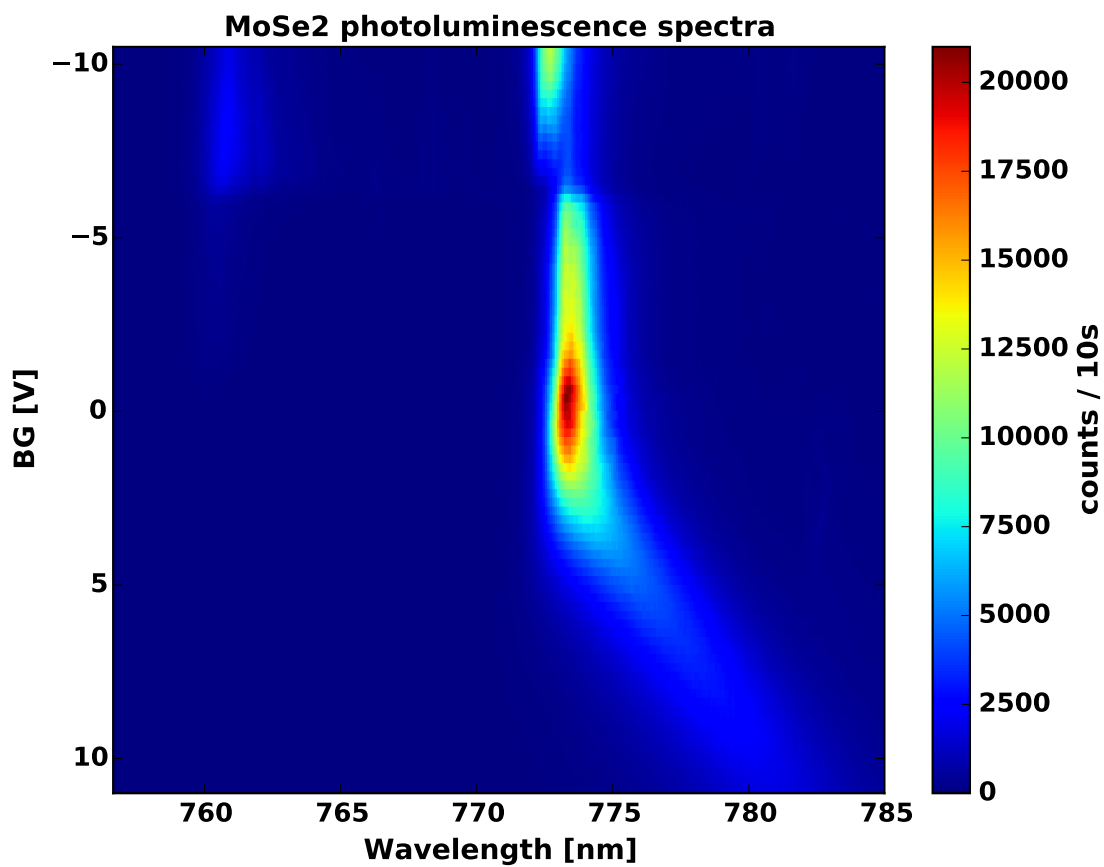


FIG. S2: Electron density dependent photoluminescence measurement of monolayer MoSe<sub>2</sub>. We observe the PL from exciton for low gate voltages  $V_g$  and from attractive polaron for all gate voltages. As  $n_e$  is increased (higher  $V_g$ ), the attractive polaron resonance broadens and shifts to higher wavelengths.

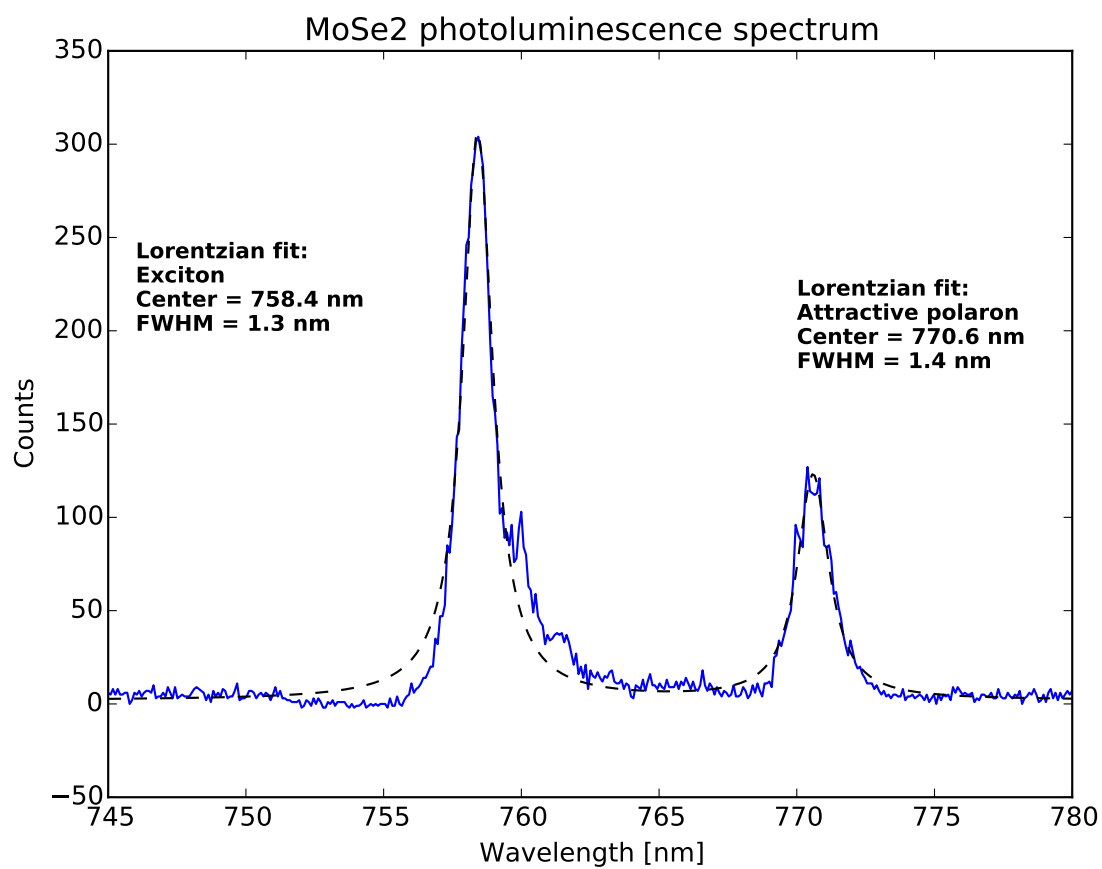


FIG. S3: PL spectrum obtained at a spot yielding the narrowest linewidth on the sample investigated in the main text. The gate voltage was chosen to maximize the exciton PL. By fitting the exciton resonance with a Lorentzian, we extract a line width of  $\simeq 2.8$  meV.

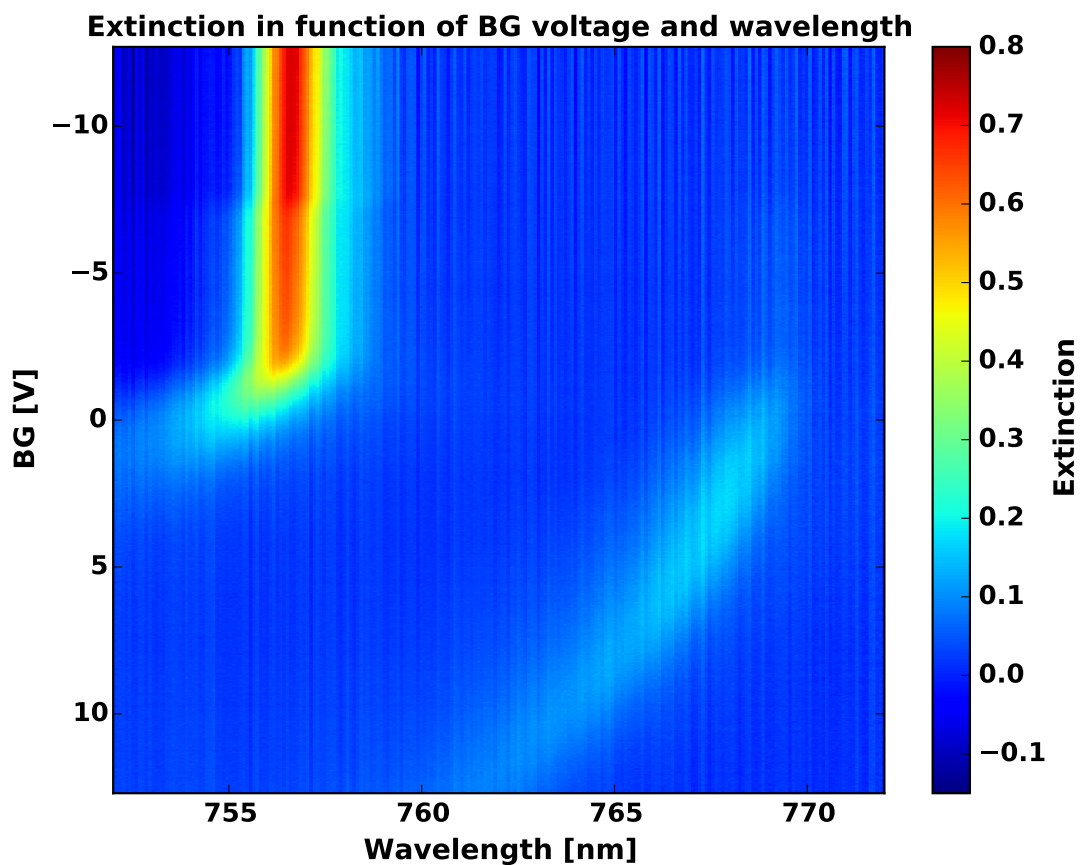


FIG. S4: Transmission spectrum of the heterostructure obtained using a broadband LED source.

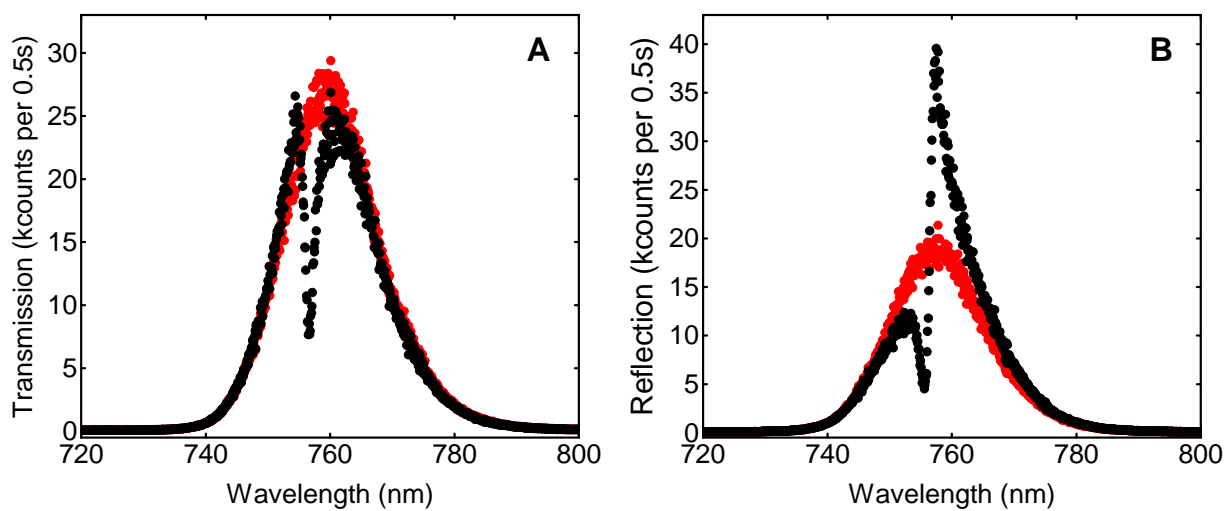


FIG. S5: Measured broadband LED transmission and reflection spectra on (black dots) and off (red dots) the MoSe<sub>2</sub> monolayer. The off MoSe<sub>2</sub> monolayer spectrum is recorded on a part of the sample having both hBN layers and the bilayer graphene.

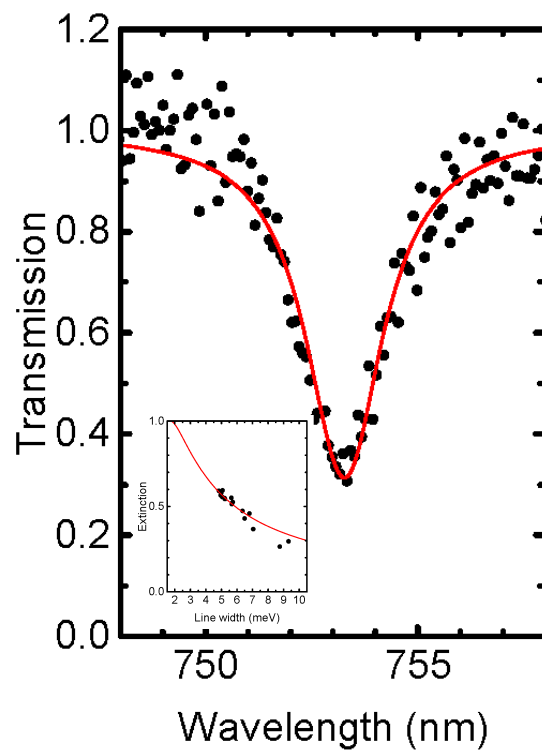


FIG. S6: The extinction of transmitted light measured on a hBN/MoSe<sub>2</sub>/hBN heterostructure on fused silica sample with full collection NA = 0.68 (without charge control). The fit corresponds to 68% extinction and a line width of 4.8 meV. The inset shows the relationship between the amount of extinction and line width measured on different spots of this sample.